A Journal of

EurJIC

European Journal of Inorganic Chemistry

ChemPubSoc Europe

Accepted Article

Title: Low cost catalysts for Water Gas Shift reaction based on CuNi over La promoted ceria

Authors: Eduardo Poggio-Fraccari, Abigail Rozenblit, and Fernando Mariño

To be cited as: *Eur. J. Inorg. Chem.* 10.1002/ejic.201800048

Link to VoR: http://dx.doi.org/10.1002/ejic.201800048

WILEY-VCH

10.1002/ejic.201800048

Low cost catalysts for Water Gas Shift reaction based on Cu Ni over La promoted ceria

Eduardo Poggio-Fraccari [a]*, Abigail Rozenblit [a], Fernando Mariño [a]

[a] Dr. Eduardo Poggio-Fraccari, Eng. Abigail Rozenblit, Dr. Fernando Mariño

Instituto de Tecnologías del Hidrógeno y Energías Sostenibles, ITHES (UBA-CONICET),

Ciudad Universitaria, Pabellón de Industrias (1428), Buenos Aires

Universidad de Buenos Aires (Argentina)

Phone number: +54 011 528 50360

E-mail: eduardoaristidespf@di.fcen.uba.ar

ABSTRACT

PEM fuel cells are of great interest for vehicular applications. A highly pure, sustainably obtained H_2 stream is desirable to use as the cell feed. The Water Gas Shift reaction (WGS) is one of the stages in which large amounts of CO, a poison for the cell anode, are removed from a bio-alcohol derived H_2 stream, before entering the cell. In this study, Cu-Ni catalysts supported on a combination of La-doped ceria solids are analyzed and proposed for the WGS reaction. The solids were prepared via the urea thermal decomposition method, with different percentages of La as a promoter of the ceria support. The metal phase is incorporated via incipient wet impregnation. Many characterization techniques have been employed in this work (BET, XRD, SEM, ICP, TPR, OSC), and a relation between the properties obtained from these studies and the solid's catalytic performance is attempted in order to determine the effect of La presence.

A mixture of both Cu and Ni was found to be the most effective active phase out of all the studied samples, having considerable activity and selectivity towards the desired reaction. Low contents of La doping on ceria enhance oxygen mobility in the lattice. From the results presented in this work it can be concluded that a commercial ceria salt containing La as its main impurity (ca. 2%) is quite convenient, given its good performance and its low market value compared to a high purity salt.

1. INTRODUCTION

The Water Gas Shift (WGS) reaction has been extensively used in industry processes since 1960. However, new non-conventional applications of hydrogen have led to a renewed interest in the reaction. Hydrogen obtained from different sources can be used as a feed stream to fuel cells. One of the most popular fuel cells is the proton exchange membrane fuel cell (PEMFC), due to its applicability to stationary and mobile uses. A sustainable H_2 stream can be obtained from the reforming of bio-alcohols [1], which is a carbon-containing raw material. Hence, a purification process must be carried out in order to reduce CO levels to meet the PEMFC requirements. One feasible catalytic purification process consists in the use of a 2-stage reactor train. The first stage is a WGS converter, in which the CO concentration is reduced from ca. 8% to 1% molar base. The second stage aims to reduce CO levels to a maximum of 20 ppm. The reactor used in this last step is a CO preferential oxidation unit (COPROX). According to Zalc and Löffler [2], the WGS reactor is expected to have the largest volume out of the two, since the intrinsic activity of WGS catalysts is low and the reaction is strongly limited by thermodynamics. Therefore, catalyst development will be focused on its performance in reaction conditions.

Recent studies on the subject have resulted in several works on WGS catalysts, which could represent an alternative to those used commercially (Fe-Cr and Cu-Zn-Al). Some authors have focused on the redox properties and the oxygen storage capacity of ceria (CeO_2), and then proposed ceria-supported noble metal catalysts [3-5] or, the less expensive ones, ceria-supported transition metal catalysts as Cu or Ni [6-9] as viable alternatives. Recently, a novel bimetallic formulation of Cu-Ni has been reported to show great performance in reaction conditions [10,11]. The redox and catalytic properties of the support can be enhanced by adding another element to the lattice, called a promoter. In the case of ceria supports, La- and Pr-containing samples have shown a higher performance than pure ceria [12-14]. In previous works, we have studied the addition of Pr to ceria supports in Cu-Ni catalysts and observed a promoting effect of redox couples Ce^{4+}/Ce^{3+} and Pr^{4+}/Pr^{3+} for the WGS reaction, concluding that the presence of Pr in small amounts (close to 5 wt.%) enhance the catalytic activity of Cu samples and the selectivity of Ni samples [15,16].

The addition of La to ceria is extensively reported in literature, given that it is the most abundant of lanthanides, and that it is a very common impurity in Cerium precursor salts. Several authors have suggested an improvement of ceria's oxygen storage capacity with the addition of La to its

lattice[17,18]. Moreover, the use of Cu and Ni catalysts supported on lanthana-doped ceria has been reported for the WGS reaction, although no composition screening was carried out [7,10].

As it was mentioned above, the WGS reactor is expected to have the largest volume out of the H_2 production-purification train of reactors and, consequently, the cost of the catalyst bed for this reactor must be considered. Therefore, the aim of the present work is twofold: (i) to study the effects of La addition to ceria supports on the catalytic performance of Cu-Ni catalysts; and (ii) to analyze the performance of a cerium commercial precursor salt, containing La as its main impurity. This commercial salt is economically attractive, since it is sold at half the market price of the high purity salt (>99%). All CeLa samples were characterized in order to obtain their redox and textural properties, and tested in WGS reaction conditions.

2. RESULTS AND DISCUSSION

2.1 Characterization of CeLa supports

The precipitation via the urea thermal decomposition method has proven to be adequate for the synthesis of several mixed-oxides precursors, such as Ce-Cu, Ni-Cu, and Zn-Cu, with high reproducibility in a single step [20]. Synthesis parameters, such as temperature or precipitation time, can modify the morphology of the resulting solid and, therefore, its surface area and redox properties. Another important parameter that has an impact on the morphology of the samples is the urea:cation ratio [26]. Even more, it was reported that morphology and surface reactivity are strongly related to CO reaction activity [22]. In the present work, three different urea:cation ratios were studied for sample CeLa5: 2:1, 10:1 and 20:1. The remaining parameters were kept unmodified. Analyzing the SEM micrographs presented in Figure 1, it can be seen that small particles form a rod-like agglomeration when the urea:cation ratio is lowest, and a quasi-spherical shape was observed in samples with higher urea:cation ratio. This result is in agreement with reports by Ji et al., which state that spherical shapes were favored when high concentrations of urea were used during synthesis [25].

It can be observed that the higher the urea:cation ratio, the lower is the resulting surface area of the annealed oxides, and the larger their particle size (estimated by BET, assuming spherical particles [23]), see Table 1. This same trend was also found by Wang and Lu for their pure ceria samples [24]. The authors claimed that during hydrolysis of urea at high concentrations, new nuclei of the precursor material tend to agglomerate along with previously formed particles, rather than forming new nuclei, resulting in grain growth. Besides, Matijevic and Hsu have reported that synthesis methods with low urea concentrations and temperatures of around 90 ºC (as used in the present work) yield a low precipitation reaction rate, which results in smaller particles. This is in agreement with the estimated particle size by the BET isotherm [2]. In summary, a low urea:cation ratio produces samples with a slightly higher surface area, but slow precipitation rates are entailed. It was concluded that a 10:1 ratio was optimal for the synthesis method, and was used for solid synthesis throughout this work.

After precipitation, solids were calcined and CeLa oxides were obtained, which were later dissolved in concentrated orthophosporic acid at room temperature. La content was measured via elemental analysis of solutions (ICP), results are reported in Table 1. As it can be seen, the values are close to the nominal ones for contents up to 15 at.%, which is in agreement with findings by Deganello and Martorana [27], but a great deviation from the targeted value is observed for CeLa50, suggesting that some La^{3+} ions did not precipitate during synthesis.

10.1002/ejic.201800048

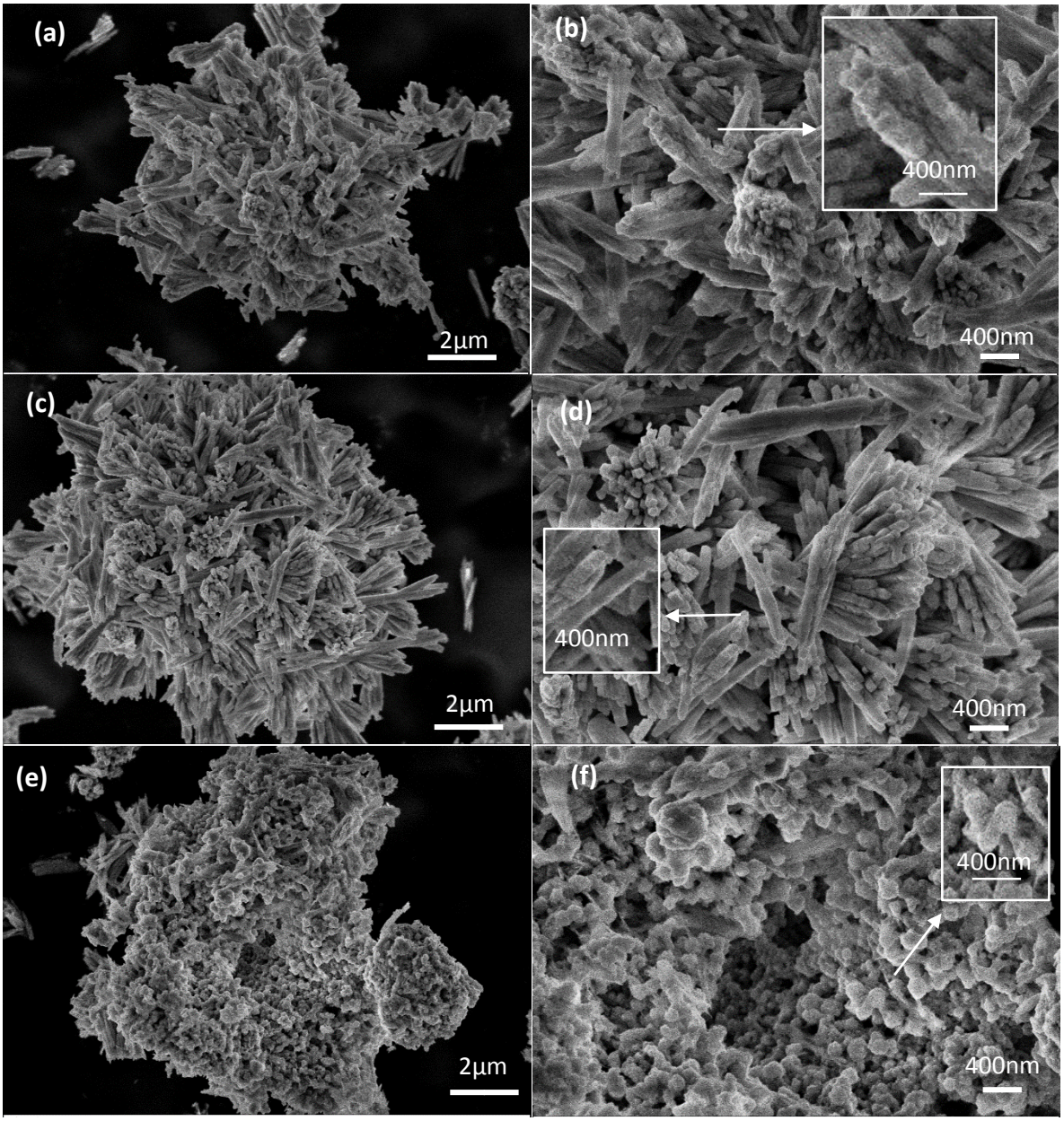

Figure 1: SEM micrographs of CeLa5 synthesized with different urea:cation ratios, left side with 20000X and right side with 50000X. (a) and (b) 2:1 ratio, (c) and (d) 10:1 ratio, (e) and (f) 20:1 ratio.

The addition of large amounts of La to ceria has been reported in literature, using more complex synthesis methods like hydrothermal precipitation with urea or citrate [17,18]. However, the main advantages of the method used in the present work are high mass yields and its simplicity, which makes it particularly attractive for scaling-up.

Table 1 also displays the BET values for CeLaX supports. As it can be seen, surface area steadily decreases as La content increases [28-30], with a marked decline in sample CeLa50, which shows almost 90% of area loss in comparison with pure ceria. The particle size estimated with BET increases slightly with La contents up to 15 at.%, whereas a significant boost is observed in CeLa50.

Table 1: ICP, BET and XRD results for CeLa samples

Samples	La content (% by ICP)	S_{BET} (m^2/g)	D_{BET} (nm)	D_{XRD} (nm)	$(D_{BET}/D_{XRD})^3$	a (mn)
CeLa0	-	110.9	7.6	8.1	0.8	0.5416
CeLa5-2:1*	ND	82.5	10.1	ND	ND	ND
CeLa5	3.9	77.8	10.7	7.8	2.6	0.5439
CeLa5-20:1*	ND	58.9	14.1	ND	ND	ND
CeLa15	14.4	63.4	13.1	6.4	8.8	0.5460
CeLa50	28.2	12.0	69.4	5.4	2120	0.5536

*: Samples with a different urea:cation ratio

XRD patterns of CeLaX samples are reported in Figure 2 (a). Fluorite CeO_2 (JCPDS No 42-1002) reflections were detected in all samples, including the one with the highest La content. This implies the existence of a solid solution for all La contents studied. Other authors have also reported a ceria-lanthana solid solution formation for La additions up to 60% using sol-gel or reverse microemulsion methods [17,18]. The incorporation of La^{3+} (ionic radii 0.106 nm) to a fluorite cell (ionic radii of Ce^{4+} ions is 0.094 nm) causes lattice expansion [31], as it is reflected in the lattice parameter "a" reported in the rightmost column of Table 1. This effect can also be noticed in Figure 2 (b), where a shift towards lower angles was observed for the (111) plane reflection. It is worth mentioning that lattice expansion may also be due to reduction of some Ce^{4+} ions to Ce^{3+} (ionic radii of Ce^{3+} = 0.114 nm) as it is discussed below, together with the XPS analysis.

10.1002/ejic.201800048

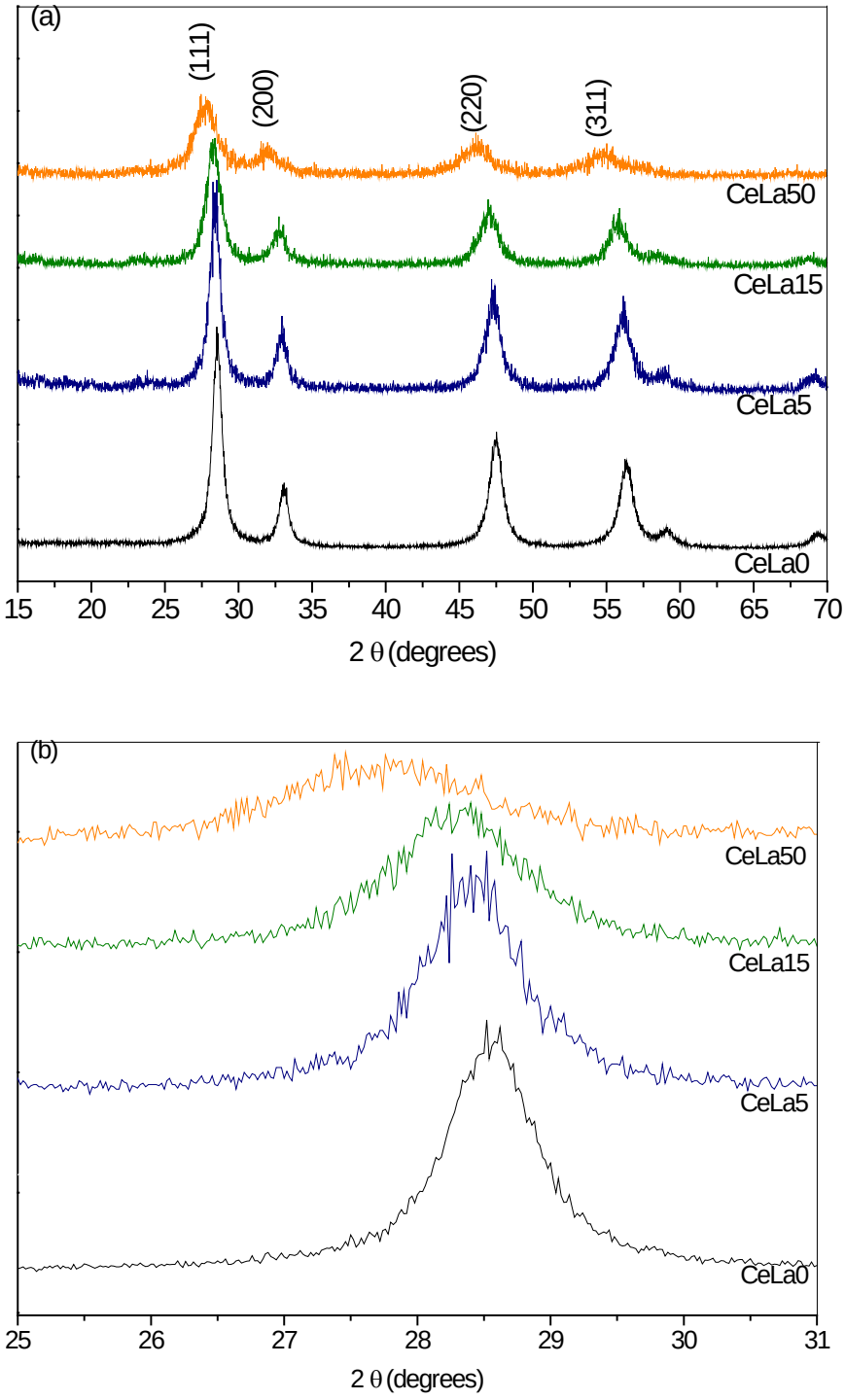

Figure 2: (a) XRD patterns for CeLa samples, (b) magnification of (111) plane.

Crystallite sizes were estimated using Scherrer's equation and the obtained values (D_{XRD}) are reported in Table 1. As La content increases, D_{XRD} decreases, indicating that the crystallite domain is smaller for samples with a higher promoter content. By the volumetric ratio of particle to crystal sizes, it can observed that crystallite agglomeration occurs with the addition of La to bare ceria, explaining the decrease in BET surface area, common to all promoted samples (Table 1).

The reducibility of solids was evaluated with temperature-programmed reduction (TPR) experiments (Figure 3). The profile of pure ceria has two distinct wide regions: α (300 - 500 ºC) ascribed to the reduction of surface ions, and β (700-1000 ºC) associated to the change of oxidation state of bulk ions [16]. Between both regions, the signal falls below baseline (arrow in the figure), implying that H_2 was physically adsorbed during first region and released in the 600-700 ºC temperature range, which is in agreement with the results of Bruce et al. [32]. Similar reduction profiles were found for ceria with low La addition (up to 5 at.%), as it is shown in Figure 3. H_2 uptake decreases for promoted samples, due to lattice replacement of Ce^{4+} ions by non-reducible La^{3+} ions, as it was concluded by previous XRD analysis and in agreement with literature [18]. Sample CeLa50 is an exception, it does not follow said trend. Moreover, some authors have reported an H_2 uptake in TPR profiles of La_2O_3 in the 500-800 ºC range, and they have assigned this H_2 consumption to the reduction of adsorbed $La_2(OH)_4CO_3$ surface species [33]. This feature might explain the H_2 consumption measured for the sample with the highest La content: this H_2 uptake is probably accounted for in the β region.

A qualitative analysis can also be made given that the TPR profiles change significantly with promoter addition. For samples with high La substitution, the α region shifts to higher temperatures. According to Zhang et al., in samples with high La contents, La^{3+} surrounds the tetravalent Ce ions in the fluorite lattice. As La^{3+} is more electronegative than Ce^{4+}, an electron transfer process occurs (O → La) hindering solid reduction [17]. Besides, in samples CeLa15 and CeLa50, regions α and β partially overlap, suggesting that bulk ions become more reducible. Wang et al. explained this feature through the enhanced oxygen mobility in the bulk resulting from the presence of large amounts of La [34]. In fact, our results show that reduction extent grows with increasing La contents. With the aid of the monolayer reduction calculation reported in a previous work, the reduction depth in the first region can be estimated [35] and values are reported in Table 2. For La contents up to 5 at.%, no significant deviations from the pure ceria profile were observed.

However, in sample CeLa15, a larger number of monolayers was reduced (i.e. more bulk ions become involved in the reduction), in agreement with the partial superimposition of α and β regions. In line with this feature, the reduced monolayer calculation was not carried out for the CeLa50 sample, because α region is not distinguishable.

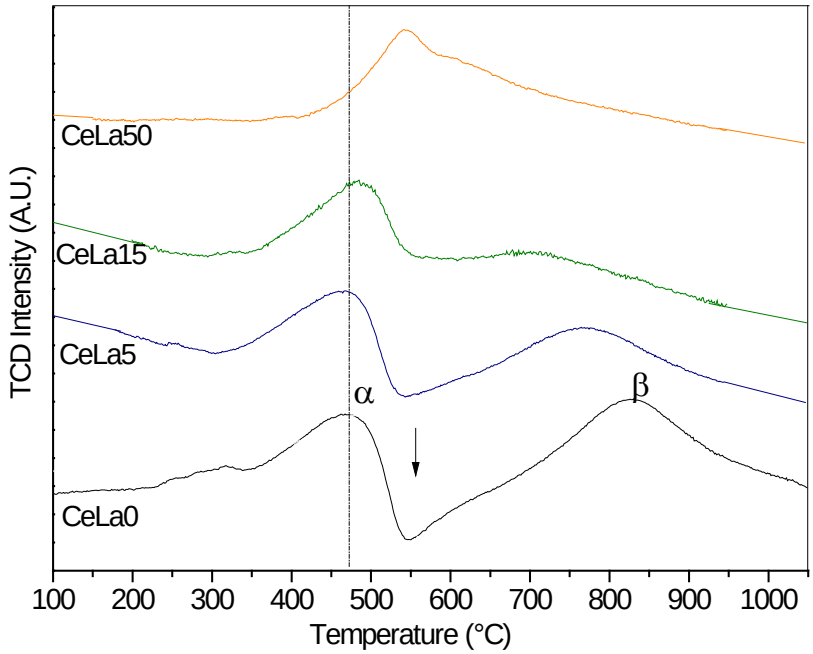

Figure 3: TPR profiles of CeLa supports

Table 2: Peak positions, H_2 uptake during TPR analysis and number of reduced monolayers

Samples	Position (°C)		H_2 uptake (μmol/g)		Monolayers reduced along α region
	α	β	α*	total	
CeLa0	471	826	360	984	0.6
CeLa5	464	765	283	522	0.7
CeLa15	484	715	408	588	1.3
CeLa50	545	-	-	690	-

*: physically adsorbed H_2 was not considered

XPS spectra of La 3d and Ce 3d regions are shown in Figure 4 (a) and (b), respectively. Intensity of La 3d region increases with promoter addition, as it was expected. From the intensity ratio of these regions, a superficial La concentration can be obtained (Table 3).

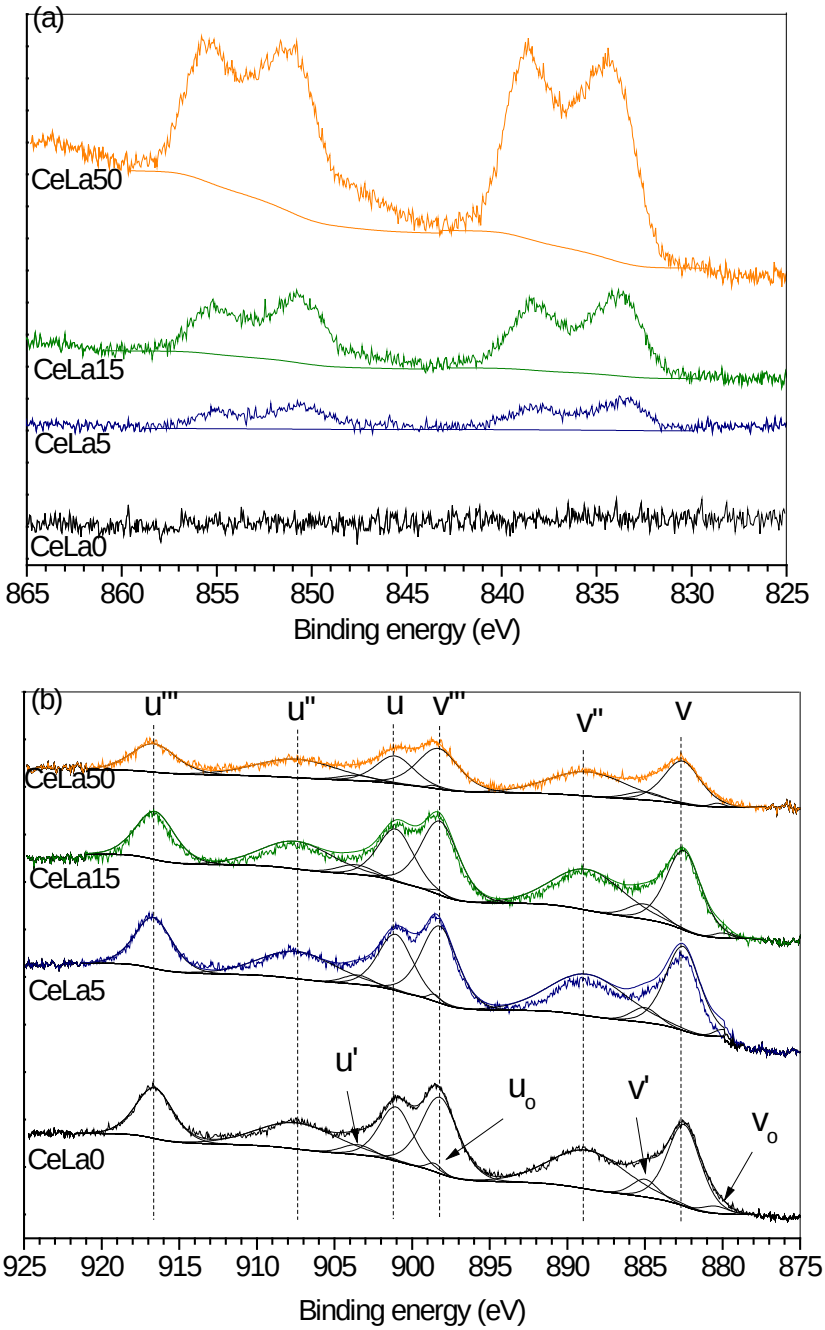

Figure 4: XPS spectra of CeLa supports: (a) La 3d region, and (b) Ce 3d region.

It can be noted that concentrations calculated with XPS are higher than those obtained by ICP (Table 1), indicating that a surface enrichment of promoter most likely takes place. An even larger difference between bulk and superficial concentration is found in the case of sample CeLa50. Other authors have also reported this same feature for their mesoporous Ce-La samples synthesized by the reverse microemulsion method [18].

Table 3: XPS results and OSC values at 400ºC for CeLa supports.

Samples	Surface La/(La+Ce) (%)	Concentration of Ce^{3+} (%)	OSC ($\mu mol_{CO2}/g$)
CeLa0	-	6.9	51.1
CeLa5	6.8	5.4	58.8
CeLa15	17.2	5.4	76.4
CeLa50	54.4	5.3	14.1

Ce 3d region was analyzed at length. It shows a more complex spectrum due to the simultaneous presence of two cations, Ce^{4+} and Ce^{3+}. Ten peaks are distinguishable in the 875 to 925 eV region, four of which are ascribable to the Ce^{3+} ion. Ce^{3+} surface fraction can be obtained from the ratio between the intensity of these four peaks to the whole spectra (Table 3). Deconvolution procedure details, such as peak assignment and constrains used, have been reported elsewhere [15]. It is worth noting that the calculated value for CeLa0 (pure ceria) is quite similar to the concentration found for a pure CeO_2 sample synthesized in a previous work, confirming the high reproducibility of the synthesis method, spectrum acquisition, and deconvolution method [35]. The superficial concentration of Ce^{3+} ions is slightly lower for La containing solids, regardless of promoter content. This could be due to a La^{3+} enrichment of samples, replacing the Ce^{3+} ions in the fluorite lattice. This same feature was also observed for CePr samples, where Pr content decreases the surface Ce^{3+} fraction of the solids [15].

Oxygen Storage Capacity (OSC) of the solids was studied to evaluate their redox properties. The values reported here are the average of several cycles of CO/Air pulses that reduce and oxidize the sample in turns (further details can be found in a previous work [15]).

Results on Table 3 show that promoter addition in moderate amounts increases the OSC of the samples, in comparison with pure ceria. Some authors explained this feature by the formation of oxygen vacancies that enhance oxygen mobility in the crystal lattice, which is evidenced by XRD and Raman spectroscopy [31]. In agreement with literature, some evidence of La^{3+} ion incorporation into the fluorite lattice was found, suggesting the existence of a non-stoichiometric oxide: (i) a shift in the (111) XRD reflection was observed, and (ii) the presence of La^{3+} ions in the surface (concluded from the analysis of XPS spectra). On the other hand, OSC of sample CeLa50 was found to be lower than that of pure ceria. This feature might be related to the severe surface area loss observed for this sample, as it is shown in Table 1. Some authors also reported that high promoter contents, close to 40-50 at.%, tend to decrease the OSC values in similar systems, such as Ce-Gd or Ce-Pr oxides [35,36].

2.2 WGS activity of CeLa supports

CeLa supports were tested for catalytic activity in a WGS reactor, in conditions described in Section 4. The main goal of this section is to study the effect La content on support activity and to select the highest performing samples to later impregnate with an active phase.

CO conversion values attained at the reactor outlet are plotted as a function of reaction temperature in Figure 5. Sample CeLa5 accomplished CO conversion values similar to those by pure ceria. However, further La addition (samples CeLa15 and CeLa50) weakens the solid's activity. The low conversion attained with sample CeLa50 can be explained by its low reducibility, low OSC values and low surface area. Analyzing sample CeLa15, there is no apparent correlation between CO conversion and redox or structural properties, since this sample is the one with highest OSC value and it presents acceptable reducibility. In order to elucidate this point, OSC was measured for samples CeLa15 and CeLa5 after having been employed in WGS activity runs (Table 4). It can be noted that the OSC of the spent CeLa15 decreases to 50 % of its original value. The OSC of spent CeLa5 also decreased, but in much smaller proportion, suggesting that oxygen mobility is more sensitive to exposure to reaction conditions for sample CeLa15.

Figure 5 also shows the activity of a Ce-La sample synthesized with a commercial Ce precursor salt containing La as its main impurity (less than 2 at.% by specification), called $Ce(La)O_{2-y}$. It

showed a similar performance to that of CeLa0 (pure ceria) indicating that precursor salt purity has no major influence on sample activity. In conclusion, samples with moderate to high La content showed no advantages regarding WGS activity, while contents lower than 5% at. appear to be more promising. $Ce(La)O_{2-y}$ and CeLa5 were found to be the most active supports, and were selected to impregnate with Cu and Ni active phases.

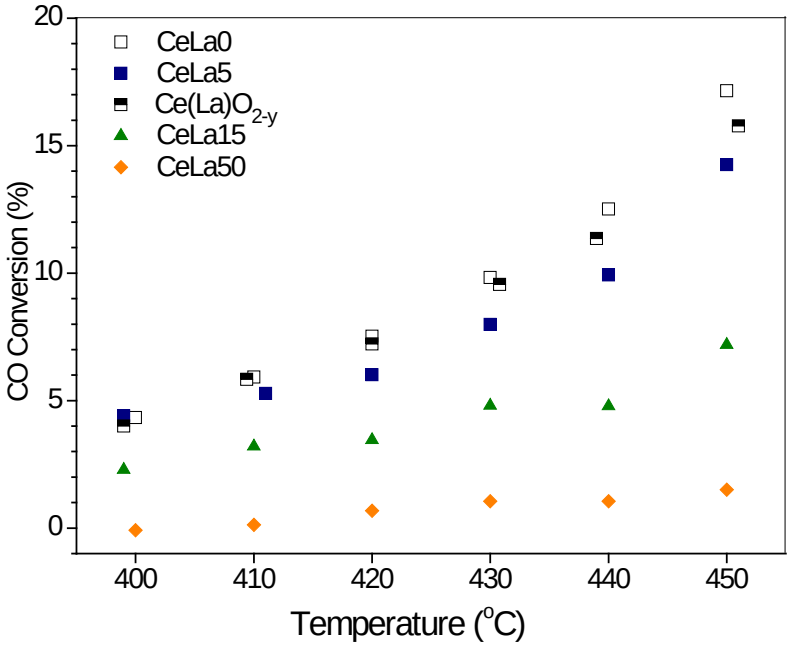

Figure 5. Bare supports performance in WGS reaction. Conditions: 240 mg of catalyst load, 85 cm^3/min of gas flow with a composition of: 8% CO, 24% H_2O and the rest is N_2.

Table 4: OSC measurements at 400 °C of fresh and spent samples

Samples	OSC ($\mu mol_{CO2}/g$)	OSC of spent samples ($\mu mol_{CO2}/g$)	OSC diminution (%)
CeLa5	58.8	41.9	29
CeLa15	76.4	34.8	55

2.3 Characterization of Cu and Ni catalysts

Figure 6 shows the reduction profiles of catalysts obtained via the impregnation of Cu and/or Ni over support samples CeLa5 and $Ce(La)O_{2-y}$ (the experimental procedure is detailed in Section 4). As it can be seen, both Cu catalysts present reduction events starting at 90 ºC, and a main peak close to 160 ºC. As it was expected, these temperatures are much lower than those observed for bare supports in Figure 3. Besides, in accordance with reports in literature, bulk CuO is reduced at approximately 300 ºC [16], suggesting that reducibility of Cu species is enhanced by the presence of a CeLa oxide. By a quantitative analysis of H_2 uptake, it can be noted that support reduction also takes place in the low temperature range, given that H_2 uptake is higher than the stoichiometric required amount to reduce all Cu^{2+} to Cu^0 (Table 5). In summary, there appears to be a synergistic effect between CeLa mixed oxides and Cu^{2+} species, which results in higher sample reducibility [38]. This feature was observed for both Cu catalysts. In fact, their profiles proved to be quite similar, indicating that reducibility did not change when a commercial Ce precursor salt was used instead of a high purity precursor salt.

TPR profiles of these Cu catalysts show at least four reduction events in the 90-220ºC range. Several authors have proposed peak assignments for the Cu-ceria system, where low temperature events are often ascribed to the reduction of highly dispersed Cu^{2+} species in close interaction with the support [7], while peaks at higher temperature are assigned to the reduction of larger Cu particles interacting less strongly with the support, or even agglomerated CuO [7,9].

Table 5: H_2 consumed in TPR experiments and corresponding theoretically amount to reduce all Cu^{2+} and Ni^{2+} to metallic state.

Samples	H_2 consumption ($mmol/g_{cat}$)	Stoichiometric H_2 consumption ($mmol/g_{cat}$)
$Cu/Ce(La)O_{2-y}$	1.06	0.63
Cu/CeLa5	1.02	0.63
$Ni/Ce(La)O_{2-y}$	0.84	0.67
Ni/CeLa5	0.69	0.67
$CuNi/Ce(La)O_{2-y}$	0.76	0.65
CuNi/CeLa5	0.71	0.65

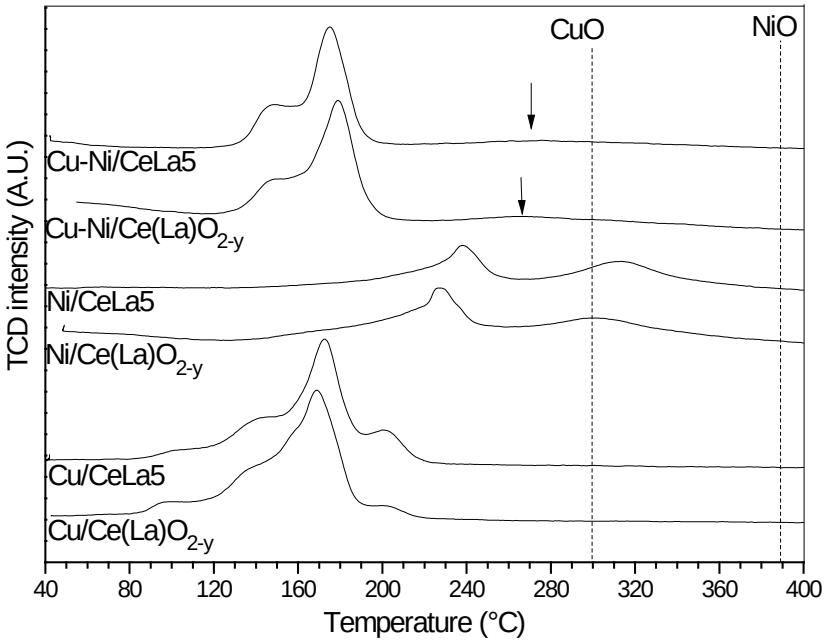

Figure 6: TPR profiles of catalysts.

Ni catalysts showed two wide reduction events in the 200-340 ºC range, before the reduction of the support (see Figure 3) and bulk NiO species takes place (marked with a dotted line in Figure 6). This might suggest that a synergistic effect also takes place in these samples. Both bimetallic samples showed reduction events in the 130-200 ºC range, similar to those of Cu solids, indicating

that reducibility of Cu^{2+} species is not significantly affected by the presence of Ni^{2+}. In addition, a very small peak can be observed at 230-240 ºC (tagged with an arrow in Figure 6), region in which pure Cu catalysts profiles do not show any H_2 consumption. It should be noted that this peak occurs in the Ni reduction region. Analyzing H_2 consumption, only a small fraction of Ni^{2+} species is reduced at this high temperature event, while the vast majority is reduced in the low temperature region along with Cu^{2+} species. This might suggest that the presence of metallic Cu (species that had already been reduced at 230 ºC) enhances the Ni^{2+} reduction taking place at 230-240 ºC, which is in agreement with previous observations of CuNi samples supported over La promoted ceria [10,16].

2.4 Catalytic activity of Cu and Ni samples

Catalysts were tested for WGS catalytic activity following the methodology described in Section 4. Figure 7 shows a plot of CO conversion as a function of the operation temperature. It is clear that Cu catalysts present very low activity for WGS in the studied temperature range. On the other hand, Ni catalysts have proven to be the most active, reaching almost 90% conversion at 450°C. These results agree with findings by other authors [3,6,38]. Bimetallic catalysts present a very acceptable activity, although conversion values are slightly lower than those of their pure Ni counterparts, which has also been observed by other authors [10,39]. However, as Ni catalysts are also active for methanation reaction, it becomes important to couple the conversion vs. temperature plot in Figure 7 with a selectivity vs. temperature plot, shown in Figure 8. Cu catalysts experiments did not yield any methane in the outlet stream, so 100% selectivity is attained with these solids.

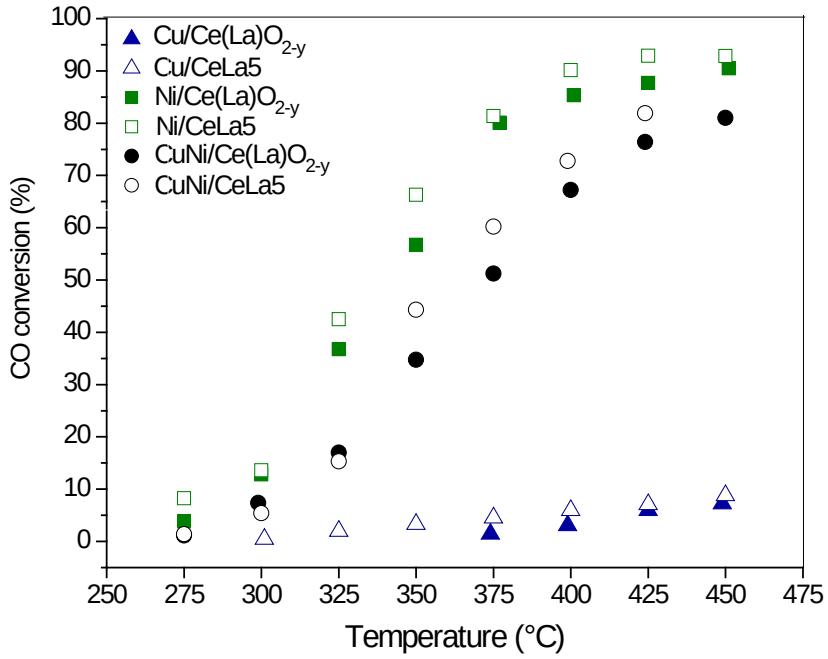

Figure 7. Cu and Ni solids catalytic performance. Conditions: 0.8 (mg min)/cm^3 with gas flow composition 8% CO, 45% H_2, 24% H_2O with N_2 as balance.

The Figure 8 shows that Ni catalysts have very low selectivity towards WGS, below 40% in all cases. When the methanation reaction occurs, three moles of H_2 are consumed for each mole of methane that is produced. Consequently, WGS must take place at least three times faster than methanation to prevent a net H_2 loss. A benchmark of 0.75 selectivity is highlighted in Figure 8, to denote the value over which H_2 net loss can be avoided. It is important to observe that Cu-Ni bimetallic catalysts achieve more than benchmark selectivity towards WGS on either support at 325°C.

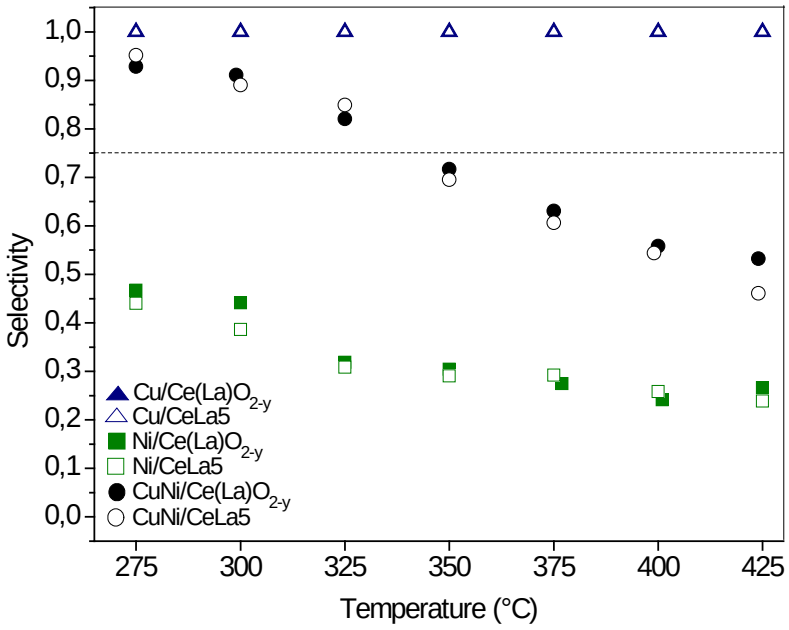

Figure 8. Catalyst selectivity towards WGS. Conditions: 0.8 (mg min)/cm^3 with gas flow composition 8% CO, 45% H_2, 24% H_2O with N_2 as balance.

In summary, Cu catalysts have shown very poor activity while Ni catalyst have an exceptionally high one, but with very low selectivity towards the desired reaction path. Bimetallic Cu-Ni catalysts seem to keep both of the metal desired features. They present much higher activity than pure Cu solids, while they are also highly more selective than their pure Ni counterparts. It is presumable that Cu presence reduces the methanation tendency, while Ni strongly enhances activity [10,16]. Reaction rate was calculated for Cu-containing samples assuming the validity of differential reactor hypothesis, i.e.: conversion values lower than 15% (and a perfect selectivity towards WGS). The values were compared with those reported in literature for similar samples and commercial catalysts in Table 6. As can be seen, values are usually obtained with feed composition avoiding WGS products CO_2 and H_2, condition which favors reaction rate. Our values included high H_2 concentration showed an acceptable performance in comparison. In fact, reaction rate for CuNi samples were similar to that obtained for High Temperature Shift catalyst.

Table 6: Comparison of WGS reaction rates reported in literature

Sample	Temperature (ºC)	Reaction rate (µmol/ gs)	Feed composition	Ref
5%Cu/CeO_2(A)	400	9.9	5%CO, 10%H_2O in N_2	40
Ni-Cu-CeO_2-IM	350	25.4	17%CO, 9%CO_2, 1%CH_4, 13%H_2, 56%H_2O, 4%N_2	41
20%Cu/$CeLaO_x$	300	13	10%CO, 20%H_2O, in He	42
20%Ni/$CeLaO_x$		35.2		
8.9%Cu/CeO_2	300	18	10%CO, 20%H_2O in He	43
Fe-Cr-Cu*	300	5.0	10%CO, 10%H_2O, 7.5%H_2, 5%CO_2 in N_2	44
5%Cu/CeLa5	300	0.3	8%CO, 24%H_2O, 45%H_2, in N_2	This study
5%Cu/Ce(La)O_{2-x}		≈0		
5%CuNi/CeLa5		3.5		
5%CuNi/Ce(La)O_{2-x}		4.9		
CuO-ZnO/Al_2O_3*	275	11.8	1.8%CO, 1.8%H_2O in He	45
5%Ni/CeO_2	275	1.6	3%CO, 3%H_2O	46
5%Cu/Ce(La)O_x	275	2.3	2%CO, 10.7%H_2O in He	37
8%Cu/CeO_2	200	0.11	7%CO, 8.5%CO_2, 22%H_2O, 37%H_2 in Ar	47
5.3%CuCe-CL	200	0.69	2%CO, 10%H_2O in He	48
Cu/ZnO/Al_2O_3*	100	0.12	1%CO, 2%H_2O	49

*commercial catalysts

2.5 Catalyst OSC

Table 6 shows OSC and OSCC values measured at 400°C of all the samples. Metal presence enhances the OSC of the support by a factor of at least 4, reaching values even 9 times higher, denoting the promoting effect of the metal on the support. Metal particles are thought to behave like entry ports for oxygen and the later migration and storage in the support lattice [50].

Cu catalysts present the lowest values of OSC and Ni catalysts present the highest ones. This trend is in agreement with the results of WGS activity reported in Figure 6. However, bimetallic samples do not follow this trend since they have the highest OSC values yet a moderate activity, suggesting that there is no direct correlation between OSC and catalytic activity. On the other hand, it is remarkable that the OSC/OSCC ratio differs significantly among samples: it is one half in the case of Cu catalysts, one third for bimetallic catalysts, and one fifth for Ni catalysts. The ratio between OSC and OSCC values is related to the ease of oxygen release from surface and bulk respectively [41]. This means that Cu catalysts, in spite of their low oxygen availability (because of their low

OSC values), are able to more readily release it due to the higher OSC/OSCC ratio (Table 7). This feature is aligned with their high reducibility, concluded from TPR experiments.

Table 7: Catalysts' OSC and OSCC measurements at 400°C

Sample	OSC ($\mu mol_{CO2}/g$)	OSCC ($\mu mol_{CO2}/g$)	OSC/OSCC
$Cu/Ce(La)O_{2-y}$	240	552	0.43
Cu/CeLa5	263	672	0.39
$Ni/Ce(La)O_{2-y}$	443	1667	0.26
Ni/CeLa5	413	1914	0.22
$Cu-Ni/Ce(La)O_{2-y}$	513	1757	0.29
Cu-Ni/CeLa5	499	1608	0.31

Comparing OSC and OSCC values with CO conversion results, it has been found that selectivity towards WGS is proportional to the OSC/OSCC ratio, and Cu-Ni bimetallic catalysts have proven to be the most suitable type of solid, balancing great activity and selectivity towards WGS. This might suggest that WGS occurs via a redox mechanism for these samples in the studied conditions, following the same trend previously found by our group for CePr bare supports [15].

3. CONCLUSIONS

A series of La-promoted ceria supports was prepared, characterized and tested for WGS activity. The highest-performing supports out of the series were selected for impregnation with metal phase,

consisting of Cu, Ni or a combination of both metals. These catalysts were characterized and tested for WGS reaction as well, and then compared with previously studied Pr-promoted catalysts.

This work leads to the conclusion that the incorporation of large amounts of La in the ceria lattice causes significant surface area loss, while enhancing the oxygen mobility in the support at the same time by creating additional vacancies. These opposing effects triggers the notion of an optimal La content, that is most probably near 5 at.%.

Urea:cation ratio used in the synthesis method was shown to be a very important factor influencing the morphology and activity of the resulting sample. A 10:1 ratio was the optimal in crystal morphology, with a high BET surface area.

The ceria support synthesized from a commercial ceria salt with La as its main impurity proved to have comparable catalytic performance and reducibility with samples CeLa0 and CeLa5. This finding has great economic implications for scaling-up: catalyst supports can be synthesized at almost half the cost employing a commercial ceria salt instead of a high purity precursor.

Cu catalysts performed poorly in the WGS reaction conditions employed in this work. Ni catalysts, although very active, favored an undesired methanation reaction, causing extremely low selectivity towards WGS reaction in whole temperature range. The analysis of metallic catalysts allowed for the conclusion that a bimetallic active phase conformed by Cu and Ni in equal parts is the most suitable combination, balancing good WGS activity and selectivity. Also, it was found that OSC/OSCC ratio correlates directly to selectivity towards WGS, suggesting that labile surface oxygen concentration is partly responsible for WGS activity.

4. EXPERIMENTAL

Cerium-lanthanum mixed oxides, hereafter called CeLaX, where X is the atomic ratio percentage (at.%) between [La] and ([La] + [Ce]), were studied throughout this work. Precursors were synthesized by the urea method [19,20], with different La contents (0, 5, 15, and 50 at.%) using $Ce(NO_3)_3.6H_2O$ (Fluka >99.0%) and $La(NO_3)_3.6H_2O$ (Aldrich 99.9%). Also, a low-cost cerium precursor salt was used, $Ce(NO_3)_3.6H_2O$ (Fluka >98.0%) with up to 2% of La as its main impurity. The ceria sample made with this salt is called $Ce(La)O_{2-y}$. Salts were dissolved and diluted

separately in distillate water and then mixed together with a 2 M urea solution, keeping a total cation concentration of 0.1 M and a urea concentration in solution of 1 M. The urea concentration was also screened between 0.2 M and 2 M in solution, in order to study the influence of this agent during synthesis. For these tests, the La content was kept at 5% at. This resulted in samples prepared with 2:1 and 20:1 urea:cations ratio, hereafter called, CeLa5-2:1 and CeLa5-20:1 for 2:1 and 20:1 ratio, respectively. In all cases, the urea and cations solution was aged in a thermostatic bath at 90°C for 24 hours. Finally, after centrifuging and washing three times, a white-colored precursor was obtained. The samples were dried in a stove at 70 ºC overnight. Calcination of samples was conducted from RT to 450°C with a 10°C/min ramp, maintaining this final temperature for 5 hours. Samples obtained in oxide form were dissolved in 10 ml of orthophosphoric acid and analyzed by ICP-AES, in order to validate the nominal composition.

Catalysts were prepared by incipient wet impregnation of ceria-based supports, obtained as previously described, with the corresponding metal salts: $Cu(NO_3)_2.3H_2O$ (Merck 99.5%) or $Ni(NO_3)_2.6H_2O$ (Merck 99.0%). After impregnation, catalysts were dried in a stove at 70°C for 24 hours, and subsequently annealed following the same thermal treatment as the bare supports. Bimetallic samples were obtained by the same method, by mixing the Cu and Ni salts in 1:1 weight ratio. Nominal active metal load is 5 %wt. for mono and bimetallic samples.

Surface area of the solids was measured via sortometry at 77 K over a wide range of relative pressures: from 0.05 to 0.995, using an ASAP 2020 apparatus. XRD patterns were collected using the graphite-filtered Cu K_α radiation (λ= 1.5406 Å) in a Siemens D5000 powder diffractometer. XPS measurements were carried out with a multi-technical system (SPECS) equipped with a dual X-ray source of Mg/Al and a hemispheric synthesizer PHOIBOS 150. Spectra were acquired with a step energy of 30 eV using Al-K_α radiation operated at 200 W and 12 kV. The pressure of the chamber was lower than 10^{-9} mbar. The analyzed regions were Ce 3d, and La 3d. The binding energies were calibrated using the Ce^{4+} (u‴) signal at a 916.7 eV as a reference [21]. Background subtraction (Shirley) and peak fitting were performed using a commercial software CasaXPS® v2.3.15. SEM micrographs were acquired with a Zeiss microscope Zupra 40 model, equipped with Gemini Column and field electron emission. Temperature-Programmed Reduction experiments were performed in a Micromeritics Auto Chem II 2920 instrument equipped with TCD detector a coupled to a Pfeiffer vacuum mass spectrometer. A flow of H_2/Ar stream (4% H_2, 50 cm^3/min)

was passed over 30 mg of the catalytic samples (120 mg in the case of bare supports), while operation temperature was raised from RT to 400°C (1050°C for supports) using a rate of 10 ºC/min. Prior to TPR tests, the samples were treated at 450ºC for 1 hour under air flow to clean the surface. Oxygen storage capacity (OSC) measurements were performed by injecting alternating pulses of CO and Air at 400°C using the Micromeritics Auto Chem II 2920 instrument previously described, and following the CO, CO_2 and O_2 signals by mass spectrometry.

Activity tests were conducted in a fixed bed reactor with a contact time of 0.8 (mg min)/cm^3, with gas composed by CO (8%), H_2O (24%), H_2 (45%) and N_2 as balance in order to determine the La-content effect in catalytic performance. The bare supports were also tested in WGS reaction. However, the conditions were changed in order to obtain higher CO conversions: 240 mg of catalyst, 85 cm^3/min (contact time equal to 2.8 (mg min)/cm^3) with a gas stream composition CO (8%), H_2O (24%) and N_2 as balance.

Before each analysis, the fresh samples which are Cu and/or Ni oxides over the CeLa oxide support, were reduced during 0.5 h in a H_2 stream (50% of H_2 in N_2) at the highest reaction temperature in order to obtain metallic active phase, Cu^0 and/or Ni^0. The catalytic performance was evaluated at several temperatures in the range 250-450°C. At the reactor outlet, analysis of non-converted CO and gaseous products was performed with a Hewlett Packard HP 6890 gas chromatograph, equipped with a TCD detector. Reported values of CO conversion correspond to steady state values.

6. ACKNOWLEDGEMENTS

The authors thank the University of Buenos Aires and CONICET for their financial support.

7. CONFLICT OF INTEREST

The authors declare no conflict of interest.

9. KEYWORDS: Water Gas Shift; Ce; La

10. REFERENCES

[1] J. Comas, F. Mariño, M. Laborde, N. Amadeo, Chem. Eng. J. **2004**, 98, 61-68.

[2] J. Zalc, D. Löffler, J. Power Sources **2002**, 111, 58-64.

[3] M. Gonzalez-Castaño, R. Ivanova, M. Centeno, J. Odriozola, J. Catal. **2014**, 314, 1-9.

[4] B. Caglayan, A. Aksoyku, Cat. Comm. **2011**, 12, 1206-1211.

[5] R. Jain, A. Poyraz, D. Gamliel, J. Valla, S. Suib, R. Madic, Appl. Catal. A: Gen. **2015**, 507, 1-3.

[6] S. Senanayake, J. Evans, S. Agnoli, L. Barrio, T. Chen, J. Hrbek, J. Rodriguez **2011**, 54, 34-41.

[7] X. Qi, M. Flytzani-Stephanopoulos, Ind. Eng. Chem. Res. **2004**, 43, 3055-3062.

[8] E. Saw, U Oemar, M. Ling, H. Kus, S. Kawi, Catal. Sci. Technol. **2016**, 6, 5336-5349.

[9] Z. Ren, F. Peng, B. Chen, D. Mei, J. Li , Int. J. Hydro. Energy **2017**, 42, 30086-30097.

[10] A. Jah, D. Jeong, W. Jang, Y. Lee, H. Roh, Int. J. Hydro. Energy **2015**, 40, 9209-9216.

[11] E. Saw, U. Oemar, X. Tan, Y. Du, A. Borgna, K. Hidajat, S. Kawi, J. Catal. **2014**, 314, .32-46.

[12] V. Rico-Pérez, E. Aneggi, A. Bueno-López, A. Trovarelli, Appl. Catal. B: Environ. **2016**, 197, 95-104.

[13] S. Parres-Escalpez, M. Illán-Gómez, C. Salinas-Martínez de Lecea, A. Bueno-López, Appl. Catal. B: Environ. **2010**, 96, 370-378.

[14] M. Małecka, L. Kepinski, W. Mista, Appl. Catal. B: Environ. **2007**, 74, 290-298.

[15] E. Poggio-Fraccari, F. Mariño, M. Laborde, G. Baronetti, Appl. Catal A: Gen. **2013**, 460, 15-20.

[16] E. Poggio-Fraccari, P. Giunta, G. Baronetti, F. Mariño, Reac. Kinet. Mech. Cat., **2017**, 121, 607:628.

[17] B. Zhang, D. Li, X. Wang, Catal. Today **2010**, 158, 348-353.

[18] S. Liang, E. Broitman, Y. Yanan, A. Anmin, G. Veser, J. Mater. Sci. **2011**, 46, 2928-2937.

[19] M. Jobbagy, F. Mariño, B. Schonbrod, G. Baronetti, M. Laborde, Chem. Mater. **2006**, 18, 1945-1950.

[20] M. Jobbagy, C. Sorbello, E. Sileo, J. Phys. Chem. C **2009**, 113, 10853-10857.

[21] E. Poggio, M. Jobbágy, M. Moreno, M. Laborde, F. Mariño, G. Baronetti, Int. J. Hydr. Energ. **2011**, 36, 15899–15905.

[22] Z. Wu, M. Li, S. Overbury, J. Catal. **2012**, 285, 61-73.

[23] F. Mariño, G. Baronetti, M. Laborde, N. Bion, A. Le Valant, F. Epron, D. Duprez, Int. J. Hydro. Energy **2008**, 33, 1345–1353.

[24] H. Wang, C. Lu, Mat. Res. Bull. **2002**, 37, 783-792.

[25] P. Ji, M. Xing, S. Bagwasi, B. Tian, F. Chen, J. Zhang, Mat. Res. Bull. **2011**, 46, 1902-1907.

[26] E. Matijevic, W. Hsu, J. Coll. Inter. Sci. **1987**, 118, 506-523.

[27] F. Deganello, A. Martorana, J Sol. Ste. Chem. **2002**, 163, 527-533.

[28] A. Bueno-López, K. Krishna, M. Makkee, J. Moulijn, J. Catal. **2005**, 230, 237-248.

[29] S. Bernal, G. Blanco, G. Cifredo, J. Pérez-Omil, J. Pintado, J. Rodríguez-Izquierdo, J. Alloy Comp. **1997**, 250, 449-454.

[30] H. Li, G. Lu, Y. Wang, Y. Guo, Y. Guo, Catal. Commun. **2010**, 11, 946-950.

[31] L. Katta, G. Thrimuthulu, B. Reddy, M. Muhler, W. Grünert, Catal. Sci. Tech. **2011**, 1, 1645-1652.

[32] L. Bruce, M. Hoang, A. Hughes, T. Turney, Appl. Catal. A: Gen., **1996**, 134, 351-362.

[33] S. Bernal, E. Blanco, F. Botana, R. García, F. Ramirez, J. Rodríguez-Izquierdo, Mater. Chem. Phys., **1987**, 17, 433-443.

[34] Y. Wang, S. Liang, A. Cao, A. Thompson, G. Veser, Appl. Catal. B: Environ. **2010**, 99, 89-95.

[35] U. Hennings, R. Reimert, Appl. Catal. A: Gen. **2007**, 325, 41-49.

[36] S. Rossignol, C. Descorme, C. Kappestein, D. Duprez, J. Chem. Mater. **2001**, 11, 2587-2592.

[37] Y. Li, Q. Fu, M. Flytzani-Stephanopoulos, Appl. Catal. B: Environ. **2000**, 27, 179-191.

[38] M. Ang, U. Oemar, Y. Kathiraser, E. Saw, C. Lew, Y. Du, A. Borgna, S. Kawi, J. Catal. **2015**, 329, 130-143.

[39] V. Shinde, G. Madras, Appl Catal B: Environ, **2012**, 123, 367-378.

[40] P. Tepamatr, N. Laosiripojana, S. Charojrochkul, Appl. Catal. A: Gen. **2016**, 523, 255-262.

[41] A. Jha, D. Jeong, W. Jang, Y. Lee, H. Roh, Int. J. Hydro. Energy **2015**, 40, 9209-9216.

[42] J-H. Lin, P. Biswas, V. Guliants, S. Misture **2010**, 387, 87-94.

[43] O. Thinon, F. Diehl, P. Avenier, Y. Schuurman, Catal. Today **2008**, 137, 29-35.

[44] L. Zhang, X. Wang, J.M. Millet, P.H. Matter, U.S. Ozkan, Appl. Catal. A: Gen. **2008**, 351 1–8.

[45] H. Kusar, S. Hocevar, J. Levec, Appl. Catal. B: Environ. 2006, 63 194–200.

[46] S. Hilaire, X. Wang, T. Luo, R. Gorte, J. Wagner, Applied Catalysis A: Gen. **2001,** 215**,** 271–278.

[47] N.A. Koryabkina, A.A. Phatak, W.F. Ruettinger, R.J. Farrauto, F.H. Ribeiro, J. Catal. 2003, 217, 233-239.

[48] R. Si, J. Raitano, N. Yi, L. Zhang, S. Chan, M. Flytzani-Stephanopoulos, Catal. Today **2012**, 180, 68-80.

[49] H. Sakurai, A. Ueda, T. Kobayashi, M. Haruta, Chem Comm. **1997**, 271–272.

[50] J. Santos-Moura, J. da Silva Lima Fonseca, N. Bion, F. Epron, T. de Freitas Silva, C. Guimaraes Maciel, J. Assaf, M. do Carmo Rangel, Catal. Today **2014**, 228, 40-50.

10.1002/ejic.201800048

TABLE OF CONTENTS

FULL PAPER

The study of the samples showed that lanthanum incorporation in ceria up to 5 at.% enhances redox and textural properties including that La-containing Ce precursor salt which has the half price market value than high purity salt usually employed. The CuNi catalysts synthesized over this support presented an acceptable combination of activity-selectivity performance.

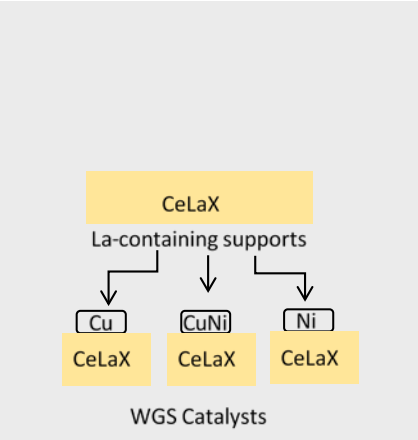

Eduardo Poggio-Fraccari, Abigail Rozenblit, Fernando Mariño*

Page No. 1 – 25.

Low cost catalysts for Water Gas Shift reaction based on CuNi over La promoted ceria